

Ly α Polarisation in Thick H I Media

Hee-Won Lee¹ and Sang-Hyeon Ahn²

¹ *Department of Geoinformation Sciences, Sejong University, Seoul 143-747, Korea*

² *Korea Institute for Advanced Study, 207-43 Cheongyangri-dong, Dongdaemun-gu, Seoul 130-012, Korea*

2002 March 4

ABSTRACT

We have investigated the linear polarisation of Ly α transferred in a static, dustless, and thick plane-parallel slab that is uniformly filled with neutral hydrogen. Because the scattering phase function is characterised by the dipole type for wing scatterings of Ly α , which is in high contrast with more isotropic scattering phase function associated with resonant scatterings, the polarisation of the emergent Ly α is dominantly controlled by the number of wing scatterings before escape from the slab. When the scattering medium is extremely thick, photons emergent in the grazing direction are polarised in the direction perpendicular to the slab normal up to 12%, which coincides with the limit attained by the Thomson scattered radiation in a semi-infinite thick medium investigated by Chandrasekhar in 1960. The number of wing scatterings before escape is sensitively dependent on the product of the Voigt parameter a and the line-centre optical depth τ_0 , with which the variation of the degree of polarisation can also be explained in comparison with the Thomson scattering case. The polarisation direction is parallel to the slab normal when $a\tau_0 < 10^3$, while it is perpendicular when $a\tau_0 > 10^3$. Our simulated spectropolarimetry of Ly α from a highly thick medium is characterised by negligible polarisation around the line centre, parallel polarisation in the near wing parts and perpendicular polarisation in the far wing parts, where the polarisation direction is measured with respect to the slab normal. The polarisation flip naturally reflects the diffusive nature of the Ly α transfer process in both real space and frequency space. We also discuss the beaming effect that is associated with the parallel polarisation in the near wing parts of the emission.

Key words: line: profile – radiative transfer – polarisation

1 INTRODUCTION

In the ultraviolet band there are many resonance lines arising from the $S_{1/2} \rightarrow P_{1/2,3/2}$ transitions including CIV $\lambda\lambda$ 1548, 1551, NV $\lambda\lambda$ 1238, 1241, MgII $\lambda\lambda$ 2798, 2800, and Ly $\alpha\lambda$ 1216. These lines are found to be prominent and conspicuous in many line-emitting objects including quasars, starburst galaxies, and planetary nebulae because they are major coolants in plasmas with temperature $T \sim 10^4 - 10^5$ K. The atomic physics associated with the $S_{1/2} \rightarrow P_{1/2,3/2}$ transitions provides a nice and simple example of the quantum interferences between the excited levels.

It is well-known that the resonance scattering between two levels with $J = 1/2$ yields isotropic outgoing radiation that is completely unpolarised. This is in high contrast with the fact that a 90° resonance scattering of an unpolarised photon associated with a $J = 1/2 \rightarrow J = 3/2$ transition yields the maximum degree of polarisation $3/7$ (e.g. Stenflo 1980; Lee, Blandford & Western 1994). Stenflo (1976a, 1976b, 1980, 1994, 1996) and Lee & Blandford (1994) studied the polarisation of resonance lines.

Interesting phenomena occur when the incident radiation is scattered in off-resonance regimes, where both the polarisation and the angular distribution of the outgoing radiation are sensitively dependent on the wavelength of the incident radiation, as is illustrated by Stenflo (1980). One general result is that scattering in far off-resonance is characterised by the classical Rayleigh scattering phase function.

Being the most prominent emission features with a very small fine-structure level-splitting in the excited states of hydrogen, Ly α should be treated with more emphasis and care. Due to the small fine-structure level-splitting of hydrogen, wing scatterings of Ly α are characterised by the classical Rayleigh scattering phase function, which is the same phase function associated with the Thomson scattering. Hence, when wing scatterings of Ly α become important in a thick medium of hydrogen, we naturally expect that the Ly α line transfer may be described in a way similar to the transfer of continuum photons in a Thomson scattering medium.

Chandrasekhar (1960) investigated the polarisation of photons transferred in a very thick electron gas, where he showed the degree of polarisation reaches 11.7% for photons emergent in the grazing direction of very thick and plane-parallel media. Phillips & Mészáros (1986) also investigated in a numerical way the radiative transfer in electron clouds, for both optically thin and thick cases. They found that the photons are beamed to the direction

normal to the slab, and obtained 11.7% of polarisation confirming the work of Chandrasekhar (1960).

The vertical column density N_{HI} of normal galaxies and dwarf galaxies ranges $N_{\text{HI}} = 10^{19} - 10^{22} \text{cm}^{-2}$. The line-centre optical depth is related with the HI column density N_{HI} by

$$\tau_0 \equiv 1.41 T_4^{-1/2} \left[\frac{N_{\text{HI}}}{10^{13} \text{cm}^{-2}} \right], \quad (1)$$

where T_4 is the temperature of the medium in units of 10^4K . This implies that the Ly α line-centre optical depth $\tau_0 = 10^6 - 10^9$ for most galaxies, and therefore one needs to deal with an extremely thick medium. It appears that many galaxies found in the early universe exhibit asymmetric Ly α emission, which is supposed to be emergent from media with these high optical depths. Therefore, if the scattering medium possesses any geometrical or kinematical anisotropy, we may expect that the Ly α emission from these objects will be polarised.

A preliminary investigation of the polarisation of Ly α emission in a thick medium has been presented in Lee & Ahn (1998). They considered an anisotropically expanding and optically thick neutral medium with a Hubble-type flow, and found that the emergent Ly α photons are linearly polarised with a degree of polarisation up to 10% in the direction parallel to the slab normal. They also applied their calculation to a hemispherical shell partly obscured by an opaque component such as a disc, and showed that about 5% of polarisation may develop.

In this paper, we calculate the polarisation of Ly α in more detail with the particular attention on the polarisation direction as a function of the optical depth. Section 2 describes the configuration of our model and the Monte Carlo code. In section 3, we show the results, and explain microscopic processes of scatterings that lead to the development of Ly α polarisation, which is followed by the summary section.

2 MODEL

In a very thick medium, wing scattering plays a very important role in the transfer of resonance line photons, which is similar to a diffusion process. Previous researchers (Avery & House 1968; Adams 1972; Harrington 1973; Neufeld 1990) introduced the diffusion approximation where only wing scatterings take place during the transfer. This approximation is very efficient for the extremely thick cases with $a\tau_0 > 10^3$, where a is the Voigt parameter defined as $a \equiv \Gamma/4\pi\Delta\nu_D$, the ratio of the natural width Γ and the Doppler frequency width $\Delta\nu_D = \nu_0(v_{th}/c)$ with v_{th} and ν_0 being the thermal speed and the line centre frequency,

respectively. We introduce the dimensionless parameter x that measures the frequency shift from the line centre in units of $\Delta\nu_D$,

$$x \equiv (\nu - \nu_0)/\Delta\nu_D. \quad (2)$$

However, Ly α photons experience both core scatterings and wing scatterings and may alternate between these two types of scattering during the line transfer. A large number of core scatterings change the polarisation vector in a random way yielding an isotropic and unpolarised radiation field. Therefore, we have to consider not only wing scatterings but also core scatterings in order to compute accurately the polarisation of Ly α emergent from a very thick H I medium.

Ahn, Lee, & Lee (2000, 2001, 2002) developed a Monte Carlo code which can deal with the Ly α line transfer in thick media. They first dealt with moderate optical depths, because the diffusion approximation is not valid in this optical depth regime. They developed an accelerating scheme for the code in order to improve the computing speed, which enabled one to calculate the line transfer in extremely thick media. The code also accurately treats the partial frequency redistribution and is equipped with a subroutine that differentiates between resonant core scatterings and non-resonant wing scatterings, providing different scattering phase functions according to the type of scatterings.

In this work, we use the same Monte Carlo code, of which the description can be found in our previous work. Our code treats the scattering of Ly α photons in a manner very faithful to the atomic physics associated with the fine-structure of hydrogen. The level-splitting of $2P_{\frac{1}{2},\frac{3}{2}}$, the excited state of Ly α transition, is 10GHz, which amounts to the Doppler width of 1.34 km s^{-1} relative to Ly α . Because this is much smaller than the thermal speed of a medium with $T \geq 100 \text{ K}$, one normally neglects the $2P_{\frac{1}{2},\frac{3}{2}}$ level-splitting, treating it as a single level. Even when $T \leq 100 \text{ K}$, the level-splitting effects may be neglected in the cases where the line centre optical depth of the scattering medium is very large. This is because the escape of line photons can only be made in considerably far wings where the level-splitting is negligible.

Since we are particularly interested in the development of polarisation of Ly α , we provide the detailed description of the code about the angular redistribution and the polarisation of the scattered radiation. We adopt the density matrix formalism to describe the angular distribution and polarisation of the scattered Ly α , where the density operator is represented by a 2×2 Hermitian matrix ρ . The usual relation with the conventional Stokes parameters

I, Q, U and V is given by

$$\begin{aligned}\rho_{11} &= \frac{I+Q}{2}, & \rho_{22} &= \frac{I-Q}{2} \\ \rho_{12} &= \frac{U+iV}{2}, & \rho_{21} &= \rho_{12}^*\end{aligned}\tag{3}$$

Fig. 1 shows the model configuration adopted in this paper. We consider a static, uniform, and optically thick HI slab with the total optical thickness $2\tau_0$ along the z -axis that is chosen to be the slab normal. The completely unpolarised Ly α source is located at the origin of the coordinate system and μ is defined as the cosine of the angle between the wavevector of the emergent photon and the slab normal. We will not consider the circular polarisation because of the azimuthal symmetry assumed in this work. Therefore $V = 0$ and ρ may be regarded as a real matrix.

In our Monte Carlo code, we only consider three types of scattering of Ly α , which are resonance scattering with $S_{1/2} \rightarrow P_{1/2}$, resonance scattering with $S_{1/2} \rightarrow P_{3/2}$ and wing scattering far from both resonance transitions. At each scattering event, we compute the probability which type of scattering has occurred. The procedure for the computation of this probability is described in detail in our previous work (Ahn et al. 2000).

The incident radiation is described by the density matrix ρ and the wavevector $\hat{\mathbf{k}} = (\sin \theta \cos \phi, \sin \theta \sin \phi, \cos \theta)$, and the scattered radiation is described by the corresponding primed quantities ρ' and

$$\hat{\mathbf{k}}' = (\sin \theta' \cos \phi', \sin \theta' \sin \phi', \cos \theta').$$

We choose the polarisation vectors

$$\begin{aligned}\epsilon_1 &= (-\sin \phi, \cos \phi, 0) \\ \epsilon_2 &= (\cos \theta \cos \phi, \cos \theta \sin \phi, -\sin \theta)\end{aligned}\tag{4}$$

for an incident photon and correspondingly ϵ'_1, ϵ'_2 for the scattered photon.

With this choice of the polarisation basis and the scattering geometry shown in Fig. 1, the polarisation will develop either in the direction parallel to the slab normal (the ϵ_2 component) or in the direction perpendicular to the slab normal (the ϵ_1 component). Therefore, we may expect that the polarisation of the emergent radiation will be described completely by $P = \rho_{11} - \rho_{22}$, the difference of the diagonal elements of the density matrix, which we will call the degree of polarisation. Hence in this convention, the positive degree of polarisation means polarisation in the direction perpendicular to the slab normal, and the negative polarisation is polarisation in the direction parallel to the slab normal. In this work, we refer

the polarisation direction with respect to the slab normal vector which is the symmetry axis of the scattering medium.

When a wing scattering occurs, the density matrix associated with the scattered radiation is given by

$$\begin{aligned}
\rho'_{11} &= \rho_{11} \cos^2 \Delta\phi - \rho_{12} \cos \theta \sin 2\Delta\phi \\
&\quad + \rho_{22} \sin^2 \Delta\phi \cos^2 \theta \\
\rho'_{12} &= \frac{1}{2} \rho_{11} \cos \theta' \sin 2\Delta\phi + \rho_{12} (\cos \theta \cos \theta' \cos 2\Delta\phi \\
&\quad + \sin \theta \sin \theta' \cos \Delta\phi \\
&\quad + \rho_{22} \cos \theta (-\sin \theta \sin \theta' \sin \Delta\phi \\
&\quad - \frac{1}{2} \cos \theta \cos \theta' \sin 2\Delta\phi) \\
\rho'_{22} &= \rho_{11} \cos^2 \theta' \sin^2 \Delta\phi \\
&\quad + \rho_{12} \cos \theta' (2 \sin \theta \sin \theta' \sin \Delta\phi \\
&\quad + \cos \theta \cos \theta' \sin 2\Delta\phi) \\
&\quad + \rho_{22} (\cos \theta \cos \theta' \cos \Delta\phi + \sin \theta \sin \theta')^2,
\end{aligned} \tag{5}$$

where $\Delta\phi = \phi' - \phi$.

When a given scattering is a resonance scattering associated with the transition $S_{1/2} \rightarrow P_{3/2}$, then the density matrix is obtained by the following relation

$$\begin{aligned}
\rho'_{11} &= \rho_{11} (5 + 3 \cos 2\Delta\phi) \\
&\quad + \rho_{22} [((5 - 3 \cos 2\Delta\phi) \cos^2 \theta^2 + 2 \sin^2 \theta^2] \\
&\quad - \rho_{12} 6 \cos \theta \sin 2\Delta\phi \\
\rho'_{12} &= 3\rho_{11} \sin 2\Delta\phi \cos \theta' \\
&\quad + 6\rho_{12} (\cos \theta \cos \theta' \cos 2\Delta\phi \\
&\quad + \sin \theta \sin \theta' \cos \Delta\phi) \\
&\quad + 3\rho_{22} \cos \theta (-2 \sin \theta \sin \theta' \sin \Delta\phi \\
&\quad - \cos \theta \cos \theta' \sin 2\Delta\phi) \\
\rho'_{22} &= \rho_{11} [(5 - 3 \cos 2\Delta\phi) \cos^2 \theta' + 2 \sin^2 \theta'] \\
&\quad + \rho_{22} [(5 + 3 \cos 2\Delta\phi) \cos^2 \theta \cos^2 \theta' \\
&\quad + 2 \cos^2 \theta \sin^2 \theta' + 12 \cos \Delta\phi \cos \theta \cos \theta' \sin \theta \sin \theta' \\
&\quad + 2 \cos^2 \theta' \sin^2 \theta + 8 \sin^2 \theta \sin^2 \theta')]
\end{aligned} \tag{6}$$

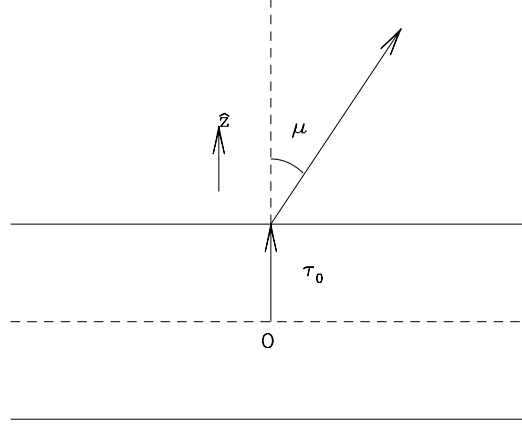


Figure 1. Configuration of the model adopted in this work. We consider the static and uniform slab with the Ly α source at the origin denoted in the figure by O . The vertical thickness of the slab is $2\tau_0$, and we define μ as the cosine of the angle between the wave vector of the emergent photon and the slab normal.

$$\begin{aligned}
 & +\rho_{12}(6 \sin 2\Delta\phi \cos^2 \theta' \cos \theta \\
 & +2 \sin \Delta\phi \cos \theta' \sin \theta \sin \theta').
 \end{aligned}$$

Finally, when the scattering is resonant with the transition $S_{1/2} \rightarrow P_{1/2}$, then the density matrix for the scattered radiation is set to be

$$\rho'_{11} = \rho'_{22} = \frac{1}{2}, \quad \rho'_{12} = \rho'_{21} = 0, \quad (7)$$

which corresponds to the isotropic and perfectly unpolarised radiation.

The angular distribution of the scattered radiation for an incident photon with $\hat{\mathbf{k}}$ and ρ is given by the trace of $\rho'(\theta', \phi', \theta, \phi)$, as is shown by Lee et al. (1997). Therefore, once the wavevector $\hat{\mathbf{k}}'$ of a scattered photon is chosen from ρ' in accordance with the scattering type, the polarisation is also determined at the same time. It is also noted that the degree of polarisation is computed only after the new density matrix is normalised so that it has a unit trace.

3 RESULTS

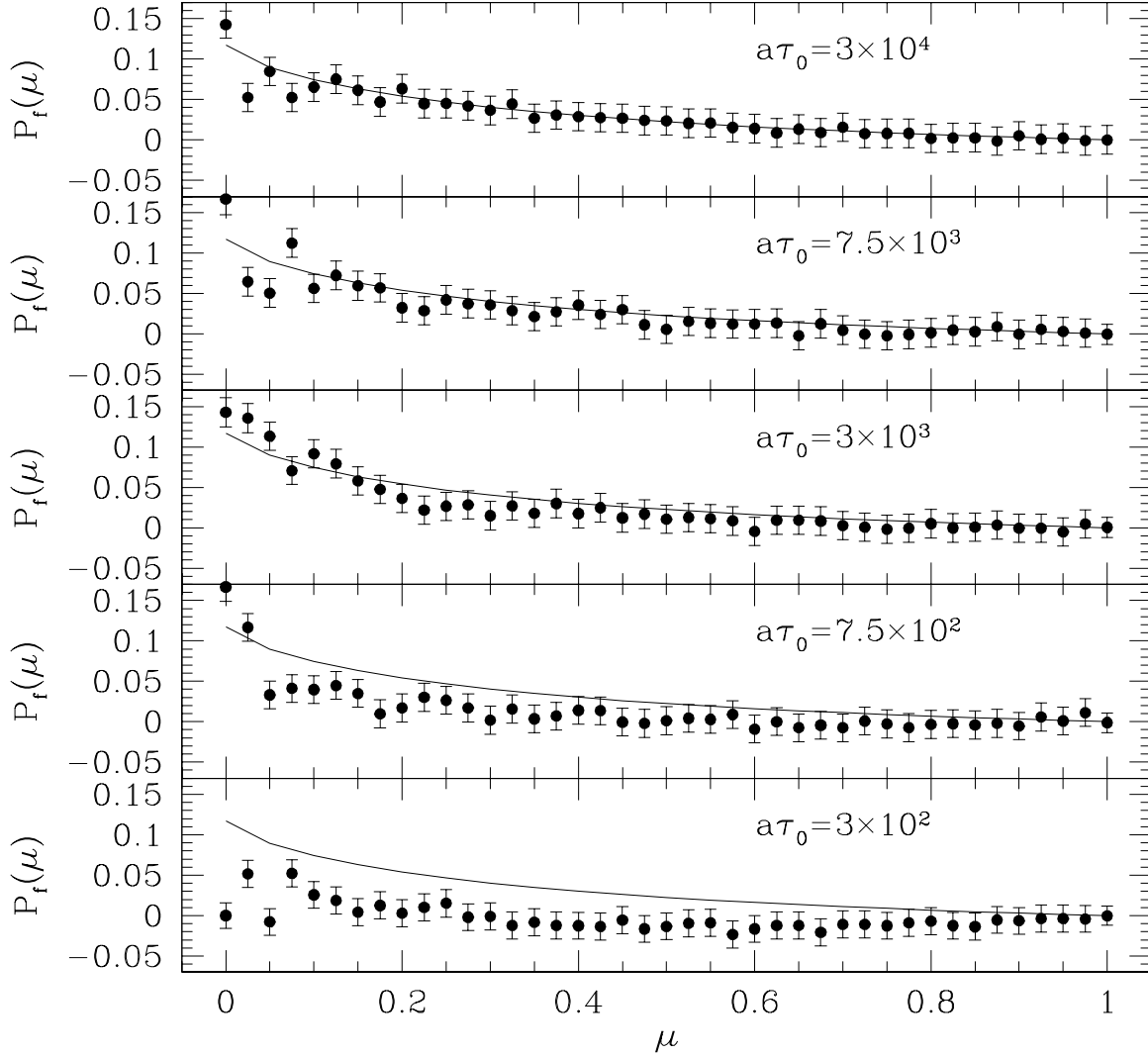


Figure 2. Polarisation of the emergent Ly α photons originated from the unpolarised source located at the midplane of the slab illustrated in Fig. 1. We show five cases with different $a\tau_0$. The solid line in each box represents the limiting behaviour for the Thomson scattering.

3.1 Degree of polarisation

We calculate the degree of linear polarisation of Ly α photons emerging from an optically thick slab with unpolarised sources distributed in its central plane. In Fig. 2, we show the linear degree of polarisation for various optical depths according to μ that represents the observer's line of sight with respect to the slab normal. In the calculations, we consider the cases where optical depths to the normal direction of the slab are $\tau_0 = 2 \times 10^4, 5 \times 10^4, 2 \times 10^5, 5 \times 10^5$, and 2×10^6 . Since we fixed $a = 1.49 \times 10^{-2}$, $a\tau_0 = 3 \times 10^2, 8 \times 10^2, 3 \times 10^3$, and

8×10^3 , respectively. In the figure, the dots with 1σ error bars represent our results and the solid lines represent the result for continuum photons transferred in a Thomson scattering semi-infinite electron cloud (Chandrasekhar 1960). We can see in the figure that the case with $a\tau_0 > 10^3$ shows good agreement with the limiting case of the Thomson scattering. We also see that the polarisation curves gradually converge to that of the Thomson scattering with a very large optical thickness as $a\tau_0$ increases.

When $a\tau_0 > 10^3$, the Ly α transfer processes are dominated by wing scatterings accompanied by the spatial transfer and Ly α photons experience a number of successive wing scatterings just before escape (Ahn et al. 2002). The number of last successive wing scatterings is determined by the scattering optical depth, τ_w at the characteristic frequency of the emergent photons, given approximately by

$$\tau_w = \frac{1}{\sqrt{\pi}} x_s, \quad (8)$$

where $x_s = (a\tau_0)^{1/3}$. They also showed that these are valid only for $a\tau_0 \geq 10^3$, when the diffusion approximation can be safely applied.

For the cases considered in this section, the characteristic wing optical depths are $\tau_w = 3.8, 5.1, 8.1, 11.0, 17.5$, respectively. According to Phillips & Mészáros (1986), the limiting behaviour is almost achieved when $\tau_e \geq 10$. The polarisation of Ly α exhibits the same limiting behaviour to that of the Thomson scattering when $a\tau_0 \geq 10^3$ or $\tau_w \geq 10$.

3.2 Spectropolarimetry

We are interested in spectropolarimetric observations for many astronomical objects. In Figs. 3-7 we show our results of the accelerated Monte Carlo calculations for the polarisation of Ly α emerging from an extremely thick hydrogen slab. The total number of photons in each simulation is 1.6×10^6 , and the frequency bin is set to be $\Delta x = 1$. For $\tau_0 = 2 \times 10^6$ we set $\Delta x = 2$ as an exception. All the quantities shown in the figures have been obtained after averaging over all emergent angles $\theta = \cos^{-1} \mu$.

In the top panel of Figs. 3-7, we show the emergent fluxes, in the middle panel the degree of polarisation P_f , and in the bottom panel the characteristic optical depth, τ_w . Treating the radiative transfer in a Thomson scattering medium as a random walk process, we convert N_w , the average number of successive wing scatterings just before escape, to the characteristic optical depth $\tau_w = \sqrt{N_w}$.

It is immediately seen that negligible polarisation develops near the line-centre. This is

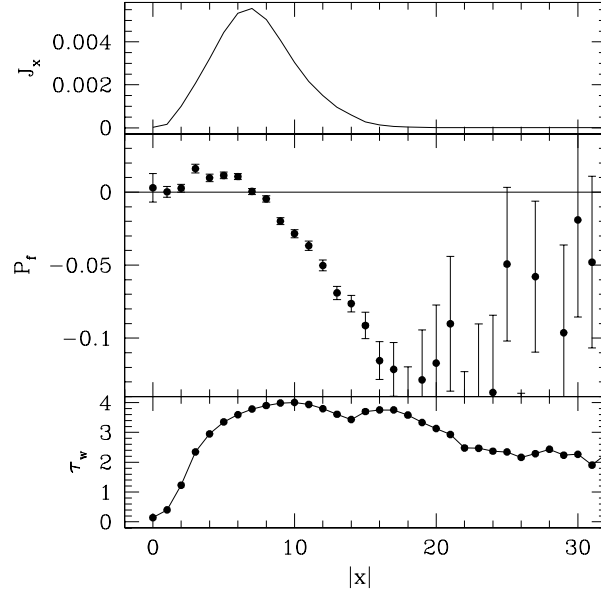


Figure 3. Simulated spectropolarimetry of Ly α emission for the unpolarised source at the central plane of a slab with the vertical optical depth from the centre of the plane $\tau_0 = 2 \times 10^4$ and the Voigt parameter $a = 1.49 \times 10^{-2}$. The top panel shows the emergent flux, the middle panel shows the degree of polarisation, and the bottom panel shows the effective wing optical depth $\tau_w^e = \sqrt{N_w}$ where N_w is the number of successive wing scatterings just before escape. All the quantities shown in the figure have been obtained after averaging over all emergent angles $\theta = \cos^{-1} \mu$.

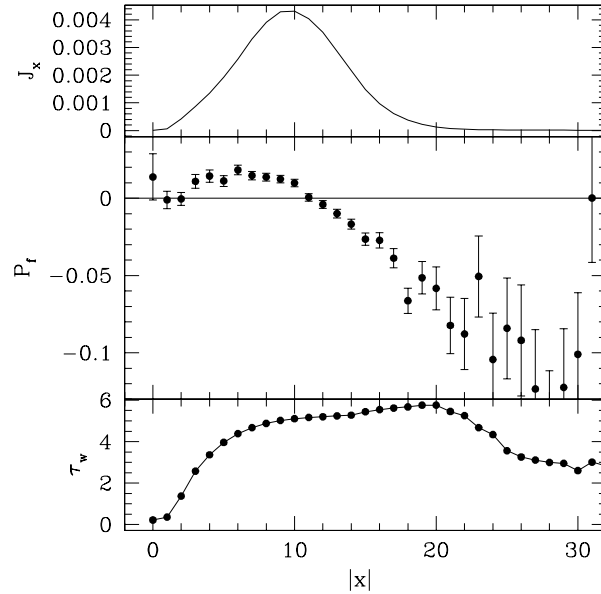


Figure 4. Simulated spectropolarimetry of Ly α from a slab with $\tau_0 = 5 \times 10^4$. All other quantities represent the same as in Fig. 3.

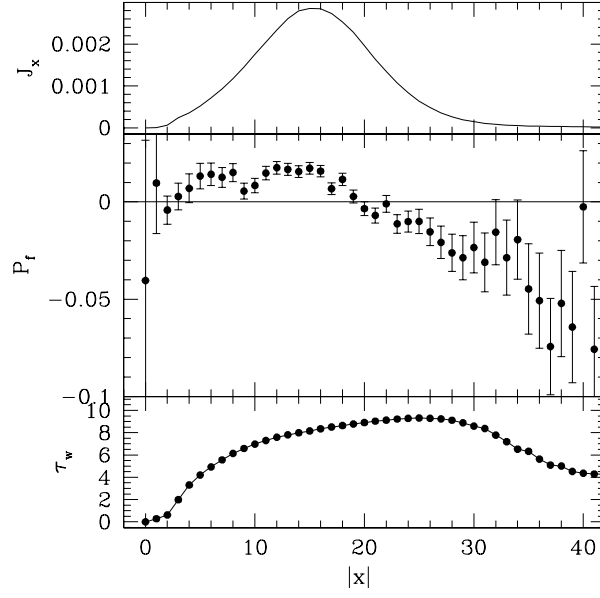


Figure 5. Simulated spectroplrimetry of Ly α from a slab with $\tau_0 = 2 \times 10^5$. All other quantities represent the same as in Fig. 3.

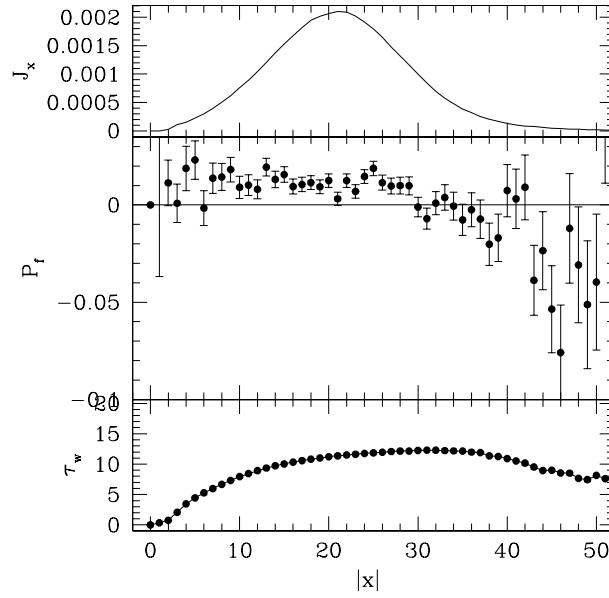


Figure 6. Simulated spectroplrimetry of Ly α from a slab with $\tau_0 = 5 \times 10^5$. All other quantities represent the same as in Fig. 3.

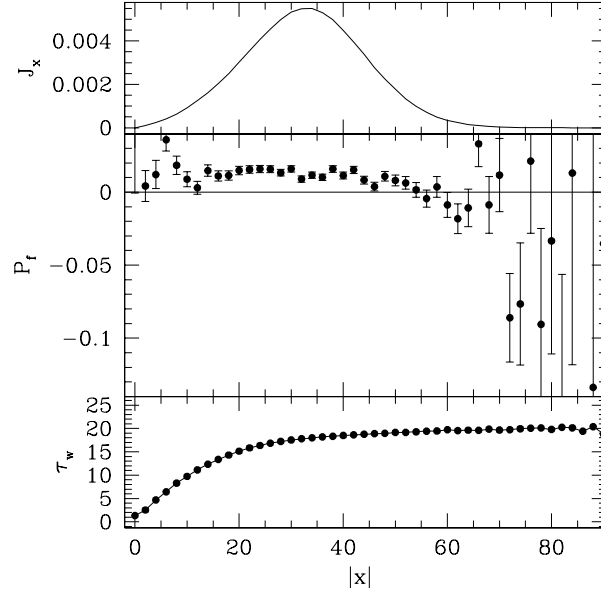


Figure 7. Simulated spectroplrimetry of Ly α from a slab with $\tau_0 = 2 \times 10^6$. All other quantities represent the same as in Fig. 3.

because line photons with frequencies near the line-centre escape through a single longest flight after a large number of core scatterings near the surface, where the local core scatterings isotropise the radiation field. The core-wing boundary frequency is approximately given by Eq.(8) with $\tau_w = 1$, or $x = \sqrt{\pi}$. Hence our results in the figure show that $P_f = 0$ at $0 \leq x \leq \sqrt{\pi}$.

The second point is that the photons filling the near wing part of Ly α emission are positively polarised, which means the electric vectors of those escaping photons tend to lie in the direction perpendicular to the slab normal. The degree of polarisation in this part is about 1%, which is smaller than the maximum value 11.7%, because they are averaged over emergent angles. It is very notable that the degree of polarisation becomes negative at far wing frequencies, which means that the polarisation direction flips from perpendicular to parallel as the frequency shift Δx from the line-centre increases.

In order for wing photons to acquire scattering numbers larger than $N_w = \tau_w^2$, they spatially diffuse much farther than τ_0 in the stage of their final series of wing scatterings. According to Ahn et al. (2002), a line photon smears out towards the slab surface via wing scatterings, and therefore the photon diffuses into the grazing direction of the slab acquiring a sufficiently large frequency shift. This means that the scattering medium is effectively very thin in the normal direction from the view point of far wing scattering Ly α photons.

Therefore, the scattering plane associated with the escaping photons nearly coincides with the slab plane, leading to the development of polarisation in the direction parallel to the slab normal. This explains the negative polarisation in the far wing part illustrated in Figs. 3-7.

On the other hand, the near wing part of the emergent profiles is contributed by photons with much larger wing scattering numbers. Therefore, a large number of wing scatterings accompanied by spatial transfer preferentially in the normal direction may cause the electric vectors of the line photons to become perpendicular to the slab normal. From this transfer process, we obtain positively polarised fluxes in accordance with our definition of polarisation direction.

Another point we can find in the figure is that the strength of the negative polarisation in the far wing regime decreases as $a\tau_0$ increases. This effect can be understood in terms of the beaming effect. Ahn et al. (2002) investigated the beaming of Ly α photons for the cases of very large $a\tau_0$, which will also be shown in the next subsection. They showed that most photons escape from the extremely thick slab-like media favourably in the direction normal to the slab plane, as is the case with an electron scattering thick cloud (Phillips & Mészáros 1986). If this is the case, the fraction of Ly α photons emergent in the direction parallel to the slab surface decrease as $a\tau_0$ increases. As a result, their contribution to negative polarisation diminishes, and eventually the degree of polarisation at the far wings becomes larger and eventually positive. Due to the beaming effect, the polarisation flip occurs farther away from the line-centre as $a\tau_0$ increases.

The polarisation of Ly α in an anisotropically expanding slab was investigated by Lee & Ahn (1998). They calculated the cases with the line-centre optical depth $\tau_0 \leq 10^5$ and the Voigt parameter $a = 4.71 \times 10^{-4}$. Their results show that the polarisation flip occurs near the line-centre, and as a result the emergent peaks are negatively polarised on average over frequencies. Because the bulk motion of the expanding slab enhances the photon escape, the polarization flip occurs at smaller optical depths than in the static medium with the same neutral hydrogen column density.

3.3 Polarisation of the total flux

Fig. 8 shows the directionality, $I(\mu)$, which is defined by $F(\mu)/\mu$. Here $F(\mu)$ is the flux along μ . We note that this was also discussed in our previous paper (Ahn et al. 2002). Ahn et al.

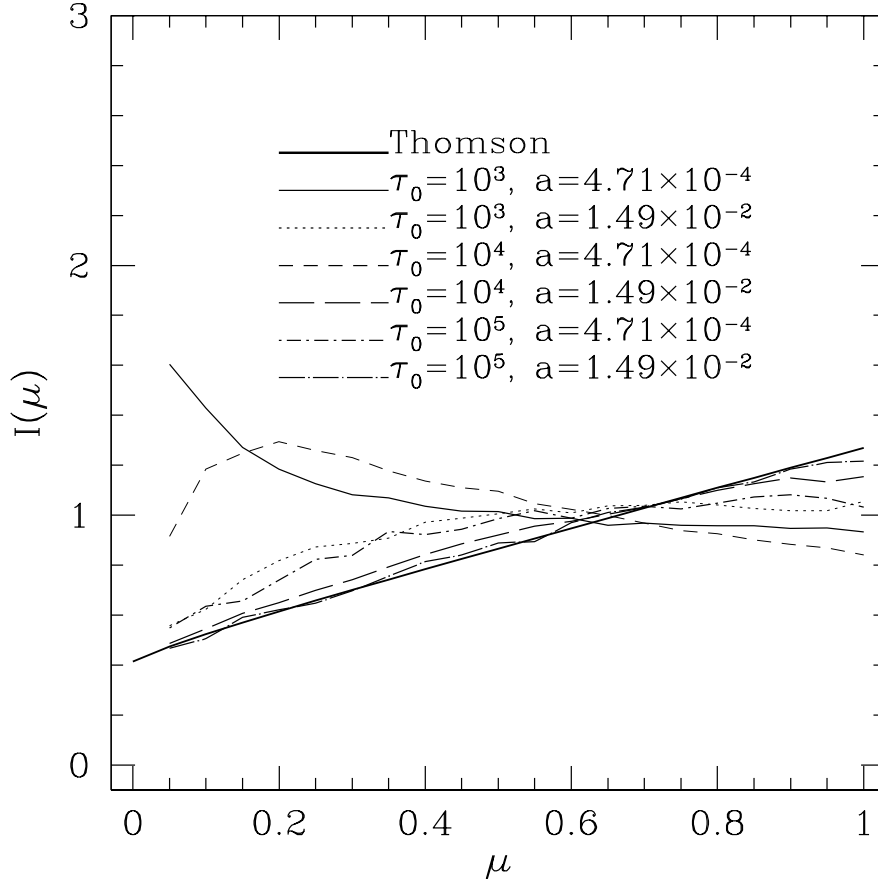


Figure 8. Directionality of emergent Ly α photons for various optical depths τ_0 and Voigt parameters a of the scattering media. We define the directionality by the flux divided by μ . The solid thick line represents the limiting behaviour of directionality for the Thomson scattering in an opaque electron cloud. We note that the curves are convex upward when $a\tau_0 \ll 10^3$ in the grazing direction. As $a\tau_0$ is greater, the directionality gradually converges to the curve for the Thomson scattering in a thick electron cloud.

(2002) discovered that the Ly α limb brightening occurs when $a\tau_0 \ll 10^3$, and that the Ly α limb darkening appears when $a\tau_0 > 10^3$.

In this subsection we show the polarisation (P_t) of total emergent flux. This quantity is obtained from the definition $P_t = \int P_f(\mu)I(\mu)\mu d\mu$, where $P_f(\mu)$ is shown in Fig. 2 and $I(\mu)$ is shown in Fig. 8.

Fig. 9 shows the degree of polarisation as a function of $a\tau_0$. Here $a\tau_0$ can be thought to be a measure of relative importance between wing scatterings and core scatterings in the line transfer. The error in P_t is simply propagated from $P_f(\mu)$. The most important thing to note in Fig. 9 is that the polarisation sign changes as $a\tau_0$. For $a\tau_0 < 750$, the polarisation direction is parallel to the slab normal, while for $a\tau_0 > 750$ it is perpendicular to it.

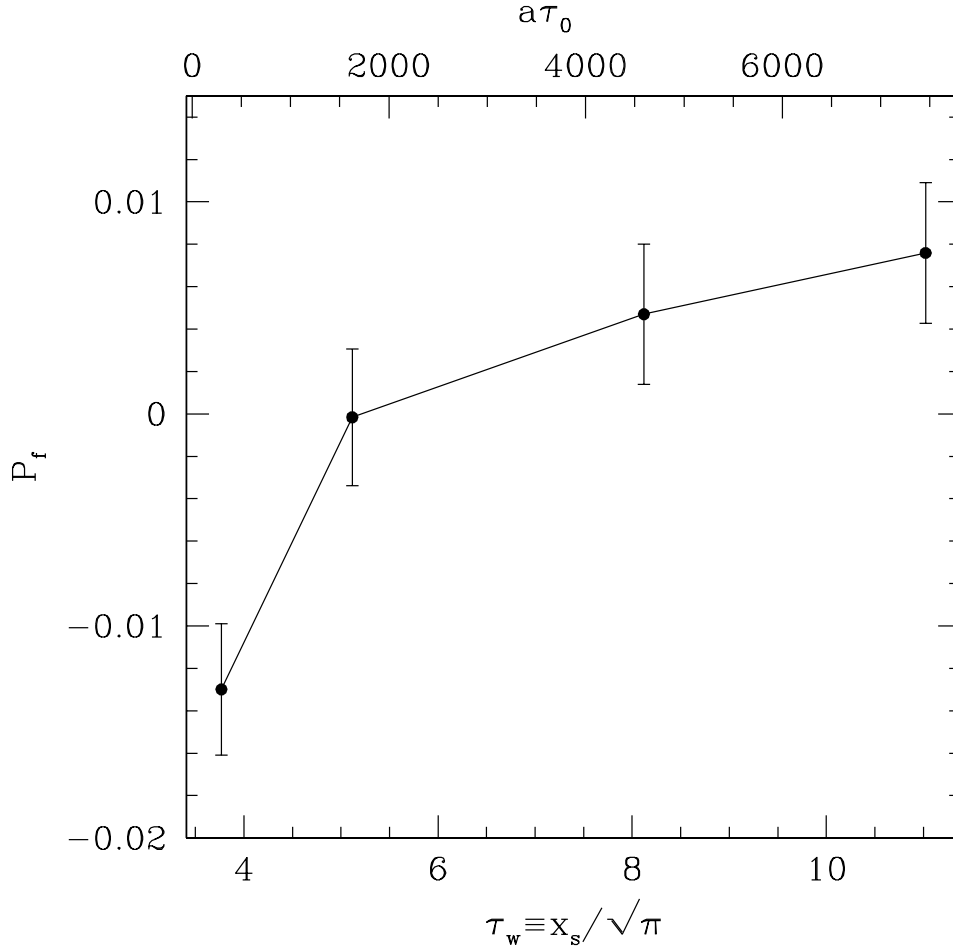


Figure 9. Degree of polarisation (P_f) when averaged over both frequency and emergent angle. We show the results for various optical depths and Voigt parameters. P_f has the negative value for $a\tau_0 < 10^3$, while the positive values for $a\tau_0 > 10^3$.

As we saw in the previous subsection 3.1, the case with $\tau_0 = 2 \times 10^4$ and $a = 1.49 \times 10^{-2}$ has the characteristic optical depth $\tau_w = 3.8$. We can understand the properties of Ly α wing scatterings by comparing with the Thomson scattering in an optically thick electron cloud with $\tau_e \approx \tau_w$, because the scattering is described by the same Rayleigh phase function and spatial diffusion dominates the transfer process.

A close examination of the curves in Fig. 2 and Fig. 5 in Phillips & Mészáros (1986) and those in Fig. 2 and Fig. 8 in this work shows that when $a\tau_0 < 10^3$ the photon flux emergent in the grazing direction of the slab surface increases as $a\tau_0$ decreases. On the other hand, the beaming of emergent Ly α is enhanced as $a\tau_0$ increases. As a result the critical frequency of the polarisation flip moves toward the larger value, which we can see in Fig. 3-7.

4 SUMMARY

We have investigated the linear polarisation of Ly α transferred in a static, dustless, and thick slab that is uniformly filled with neutral hydrogen. The polarisation behaviour of the emergent Ly α emission can be understood qualitatively by comparing with the polarisation behaviour of the Thomson scattered radiation. When the scattering medium is extremely thick or $a\tau_0 > 10^3$, photons emerging in the grazing direction are polarised perpendicular to the slab normal with the degree up to 12%, which is the same value as that of the Thomson scattered radiation in a semi-infinite thick medium (Chandrasekhar 1960).

The variation of linear polarisation with $a\tau_0$ also shows similar behaviour with that of the Thomson scattering (Phillips & Mészáros 1986). The linear polarisation of Ly α develops in the direction parallel to the slab normal when $a\tau_0 < 10^3$, while it becomes perpendicular when $a\tau_0 > 10^3$. Our simulated spectropolarimetry of Ly α shows the polarisation flip in the spectra. The linear polarisation near the line centre is almost zero. The wing parts near the line centre are polarised in the direction perpendicular to the slab normal, while the far wing parts are polarised in the direction parallel to the slab normal. The zero polarisation around the resonance frequency is caused by resonance scatterings just before escape which isotropises the electric vector of the Ly α photons. The perpendicular polarisation at the far wing parts is caused by Ly α photons preferentially emerging in the grazing direction.

The Ly α photons constituting the near wing part of the emergent peaks have large wing optical depths, and therefore they are beamed in the slab normal direction, which gives rise to positive polarisation. As $a\tau_0$ increases, the beaming effect prevents Ly α photons with far wing frequencies from emerging into the grazing direction. Therefore, the location of the polarisation flip in the Ly α line can be an important indicator of the value of $a\tau_0$.

ACKNOWLEDGMENTS

The authors thank Professor H. -M. Lee for helpful discussions and a critical reading of the original version of the paper. H.-W.L. gratefully acknowledges support from the Korea Research Foundation Grant (KRF-2001-003-D00105).

REFERENCES

- Adams T., 1972, ApJ, 174, 439
 Ahn S.-H., Lee H.-W., & Lee H.M., 2000, Journal of Korean Astronomical Society, 33, 29

- Ahn S.-H., Lee H.-W., & Lee H.M., 2001, ApJ, 540, 1
- Ahn S.-H., Lee H.-W., & Lee H.M., 2002, ApJ, 567, 922
- Antonucci R., Hurt T., & Miller J., 1994, ApJ, 430, 210
- Antonucci R., Geller R., Goodrich R.W., & Miller, J., 1996, ApJ, 472, 502
- Avery L.W., & House L.L., 1968, ApJ, 152, 493
- Chandrasekhar S., 1960, Radiative Transfer (New York: Dover)
- Harrington J.P., 1973, MNRAS, 162, L43
- Hines D.C., Schmidt G.D., & Smith P.S., 1999, ApJ, 514, L91
- Koratkar A., Antonucci R., Goodrich R.W., Bushouse H., & Kinney A.L., 1995, ApJ, 450, 501
- Koratkar A., Antonucci R., Goodrich R., & Storrs A., 1998, ApJ, 503, 599
- Lee H.-W., & Ahn S.-H., 1998, ApJ, 504, L61
- Lee H.-W., & Blandford R.D., 1997, MNRAS, 288, 19
- Lee H.-W., Blandford R.D., & Western L., 1994, MNRAS, 267, 303
- Moran E.C., Barth A.J., Kay L.E., & Filippenko A.V., 2000, ApJ, 540, L73
- Neufeld D.A., 1990, ApJ, 350, 216
- Phillips K.C., & Mészáros P., 1986, ApJ, 310, 284
- Schmidt G.D., & Hines D.C., 1999, ApJ, 512, 125
- Smith P.S., Schmidt G.D., Hines D.C., Cutri R.M., & Nelson B.O., 2000, ApJ, 545, L19
- Stenflo J.O., 1980, A&A, 1984, 68
- Stenflo J.O., 1994, Solar Magnetic Fields - Polarized Radiation Diagnostics, Kluwer, Dordrecht
- Stenflo J.O., 1996, Solar Physics, 164, 1